Energy Proceedings
Vol 57, 2025
ISSN 2004-2965

A composite gel system with CO_2 and temperature-responsive for restraining CO_2 channeling

Chuanhong Kang[1], Jixiang Guo [1*], Congcong Xu[1]

1 Unconventional Petroleum Research Institute, China University of Petroleum, Beijing, 102249, China

2 State Key Laboratory of Petroleum Resource and Prospecting China University of Petroleum Beijing, China
(*Corresponding Author: guojx003@126.com)

ABSTRACT
Carbon capture, utilization and storage (CCUS) technology is currently the most promising method for achieving low-carbon development and carbon reduction. The carbon storage and utilization part involves the injection of CO_2 into the underground. However, due to the low density and low viscosity of CO_2, gas migration often occurs during the migration of CO_2 in the formation, so suitable sealing agents are needed to repair the leakage of CO_2. A composite gel system for inhibiting CO_2 leakage was developed using the one-pot method. In this system, diethylenetriamine acts as the CO_2-responsive molecule, forming CO_2-responsive worm-like micelles with long-chain anionic surfactants. Acrylamide and a high-temperature crosslinking agent form temperature-responsive underground crosslinked gels. The response mechanism of the CO_2-responsive worm-like micelles to CO_2 is that the DETA molecules in the system come into contact with CO_2 and undergo protonation. The protonated DETA then attracts the anionic surfactant head groups through electrostatic interactions, forming a "pseudo-dipole" surfactant, and subsequently self-assembles to form worm-like micelles. When in contact with CO_2, the viscosity of these micelles will increase sharply, thus solving the problem of CO_2 channeling. The composite gel undergoes a cross-linking reaction at temperatures above 125℃, forming a non-flowing gel. This gel has excellent temperature resistance and mainly seals the weakly acidic fluid resulting from the dissolution of CO_2 in water. The research results show that during the alternating introduction of CO_2/N_2, the CO_2-responsive worm-like micelles can switch between low and high viscosities, and the CO_2 gas sealing rate can reach 99.61%. The composite gel can remain stable for 360 days at 140℃, and the water injection sealing rate can reach 98.92%. This dual-response composite gel system based on CO_2 and temperature provides technical support for CO_2 sequestration and utilization, and has broad application prospects for restraining CO_2 channeling.

Keywords: CO_2 and temperature response, composite gel system, temperature-resistant gel, CO_2 channeling, enhanced oil recovery

1. INTRODUCTION

The greenhouse effect of CO_2 has drawn widespread global attention. Many countries have actively taken measures to address the excessive emission of CO_2 in order to mitigate climate change. The current strategies mainly involve reducing the large amount of CO_2 released into the atmosphere, especially the combustion of fossil fuels in heavy industries [1]. Carbon capture, utilization and storage (CCUS) technology has become a key component in reducing carbon dioxide emissions. The CCUS framework encompasses the stages of carbon capture, transportation, utilization and storage, covering various sectors such as power, marine, oil and gas, etc. [2]. Among them, geological CO_2 utilization and storage is highly relevant to the oil and gas industry.

Low-permeability oil reservoirs in our country account for approximately 40% of the exploitable petroleum resources [3], and they have great development potential. However, how to effectively enhance the recovery rate of low-permeability oil reservoirs is an important issue currently faced by the petroleum industry. CO_2, due to its strong injectability and high oil-washing capacity, is an effective method for improving recovery rate [4-7] . With the promotion of CO_2 capture and storage technology, more and more oil reservoirs have become candidate objects for CO_2 flooding projects. Injecting CO_2 into oil reservoirs has significant economic and environmental benefits.

This is a paper for International CCUS Conference 2025 (ICCUSC 2025), May 28-29, 2025, Beijing, China.

Currently, by adopting segmented multiple fracturing technology, a reservoir fracture network can be formed during the production process of low-permeability oil reservoirs, providing channels for crude oil and increasing the initial production rate [8-10]. However, the existence of fractures is prone to cause CO_2 to prematurely break through the oil-bearing zone during the oil displacement process, resulting in gas migration and seriously affecting the sweep efficiency of CO_2 [11-14], leading to a decrease in recovery rate. At present, in the development of oil and gas fields, to solve the problem of gas migration, sealing methods are often adopted, such as gels [15-17], foams [18, 19], and water alternated gas [20, 21]. However, these methods all have some drawbacks, such as the permanent sealing of gels, the low strength and short half-life of foams, and the limited effect of water-gas alternated injection on heterogeneous oil layers. Therefore, we need to develop a new sealing method to solve the problem of gas migration in the CO_2 channeling process of low-permeability oil fields. With the development of environmentally responsive responsive materials, CO_2-responsive materials have shown great advantages due to their non-toxic, environmentally friendly, and low-cost characteristics [22, 23]. Since the Jessop team developed the CO_2-switchable solvent in 2006 [24], CO_2-stimuli-responsive surfactants, polymers, organic gels, and nano-complexes have been emerging continuously. These intelligent materials sensitive to CO_2 provide new ideas and possibilities for the development of new CO_2 gas injection sealing agents. In 2013, the Jessop research group [25] developed a new type of CO_2-responsive anionic worm-like micelle system under 60℃ conditions using $C_{18}H_{37}SO_4Na$ and N,N-dimethyl ethanolamine (DMAE). In this system, when DMAE is protonated under CO_2 stimulation, it self-assembles with the anionic surfactant $C_{18}H_{37}SO_4Na$ through electrostatic attraction to form worm-like micelles. After introducing N_2 gas, the high-viscosity micellar system can return to its initial state, and this reversible process can be repeated more than three times and the maximum viscosity of the high-viscosity micelles remains stable. Using the small molecule tertiary amine N,N,N',N'-tetramethylpropanediamine (TMPDA) and the anionic surfactant sodium dodecyl sulfate (SDS), the Feng Yujun research group [26] successfully constructed a CO_2-responsive worm-like micelle with a structure that exhibits "pseudo-dipole" characteristics. When CO_2 is not introduced, the micelles mostly present spherical or rod-like shapes, with a viscosity similar to water. When CO_2 is introduced, the tertiary amino groups at both ends of the TMPDA molecules will undergo protonation to form quaternary ammonium salts, and through electrostatic interaction, they will form "bridges" with the two SDS molecules, thereby forming worm-like micelles. During this process, the viscosity of the system increases by approximately 4000 times. After removing CO_2, the TMPDA molecules will lose protonation, and the "pseudo-dipole" structure of the entire system will disappear, presenting a low-viscosity spherical micelle state.

Although the CO_2-responsive micelle system can transform between low-viscosity and high-viscosity fluids in response to CO_2 stimulation, its viscosity loss is rapid at high temperatures, making it unable to maintain a high viscosity under high-temperature conditions.Although the CO_2-responsive micelle system can transform between low-viscosity and high-viscosity fluids in response to CO_2 stimulation, its viscosity loss is rapid at high temperatures, making it unable to maintain a high viscosity under high-temperature conditions. To enhance the thermal stability of the CO_2-responsive micelle system at high temperatures, a gel system with temperature responsiveness is combined with the CO_2-responsive micelle system to form a composite gel system. To enhance the thermal stability of the CO_2-responsive micelle system at high temperatures, a gel system with temperature responsiveness is combined with the CO_2-responsive micelle system to form a composite gel system. Under the stimulation of CO_2, the composite gel system can form worm-like micelles, and the increase in temperature will also cause the composite gel system to undergo cross-linking reactions to form a gel with viscoelastic properties. Under the stimulation of CO_2, the composite gel system can form worm-like micelles, and the increase in temperature will also cause the composite gel system to undergo cross-linking reactions to form a gel with viscoelastic properties. This dual-response composite gel system based on CO_2 and temperature provides technical support for CO_2 sequestration and utilization, and has broad application prospects, especially in suppressing CO_2 channeling.

2. *MATERIAL AND METHODS*

2.1 Materials

Nonionic polyacrylamide, with a relative molecular mass of 1.2×10^7 Da, industrial grade, produced by Henan Tianheng Water Purification Materials Co., Ltd.; diethylenetriamine, sodium oleate, hydrophilic gasphase nano-silica, hydrophobic nano-silica, acrylamide, polyethyleneimine (PEI), 2,2'-azidoisodibutylamine dihydrochloride (V50), analytical purity, produced by Shanghai Maclin Biochemical Technology Co., Ltd.; CO_2, N_2, >99.99%, produced by Beijing Jinggao Gas Co., Ltd. The experimental water was the formation water from the oilfield site, with a salinity of 2.11×10^5 mg/L.

2.2 Experimental method

2.2.1 Preparation of dual-response composite gel system

9.1 wt.% of sodium oleate (NaOA) and 5.4 wt.% of diethylenetriamine (DETA) were added to deionized water. Using a magnetic stirrer at room temperature (25℃), the mixture was stirred at a speed of 400 r/min for 60 minutes to obtain a yellow transparent solution. This system is a CO_2 worm-like micellar system. Then, add 6 wt.% acrylamide, 0.5 wt.% polyacrylamide and 0.2 wt.% polyethyleneimine, and finally add 0.01 wt.% 2,2'-azodiisobutyronitrile dihydrochloride. Stir at a speed of 400 r/min for 30 minutes to obtain the CO_2 and temperature-responsive composite gel system. The CO_2 response involves bubbling CO_2 into the composite gel system to transform the system into a uniform and transparent one with significant viscoelasticity, and let it stand for 24 hours; the temperature response involves placing the composite gel in a 140℃ oven for 12 hours to obtain a non-flowing gel.

2.2.2 CO_2 response test of the composite gel system

The conductivity changes and pH value changes of the composite gel system solution in the response were measured using the DDSJ-308A Leimag conductivity meter and the PHSJ-3F Leimag pH meter. The samples that had not responded to CO_2 were prepared and placed under a constant temperature of 25℃. CO_2 was continuously bubbled into the solution at a rate of 80 mL/min for 2 minutes. The conductivity and pH value were measured every 10 seconds.

2.2.3 Test of rheological properties of composite gel system

The rheological properties of the composite gel system were evaluated using the HAAKE MARS III rheometer. The viscosity test rotor used was CC24 Ti. The test conditions were 25℃ and 7.34 s^{-1}. The influence of CO_2 on the viscosity of the composite gel system was evaluated by measuring the changes in viscosity with the time of CO_2 introduction and the changes in viscosity when the system was alternately introduced with CO_2/N_2. The solution was continuously bubbled with CO_2 at a rate of 80 mL/min for 2 minutes, and the viscosity was measured once. Then, N_2 was continuously bubbled into the system at a rate of 100 mL/min for 1 hour, and the viscosity of the system was measured once.

2.2.4 Characterization of CO_2 and temperature responses

The hydrogen changes in the system during the response to CO_2 were analyzed by ^{1}H-NMR spectroscopy. DETA, NaOA, and NaOA/DETA were respectively dissolved in heavy water (D_2O). Then, a portion of the DETA heavy water solution and the NaOA/DETA heavy water solution were bubbled with CO_2. The samples were then analyzed by ^{1}H-NMR spectroscopy. To characterize the in-situ reaction process of the composite gel system from solution to gel formation, a Bruker Invenio S (Bruker Optics, Ettlingen, Germany) spectrometer was used to characterize the changes in the characteristic groups of the composite gel system during the cross-linking reaction of the solution to form a gel as the temperature increased. The test was conducted in a N_2 atmosphere with a heating rate of 5 ℃/min, and the spectra were recorded in the range of 4000 - 600 cm^{-1}.

2.2.5 DSC analysis of the composite gel system

The 204-F1 type DSC differential scanning calorimetry analyzer was used to analyze the composite gel system samples. The samples used in the experiment were undried gel samples, aiming to determine the actual temperature resistance performance of the composite gel. The scanning rate of the experiment was 10 °C/min, and the temperature range was 50 to 250°C. By comparing the absorption peaks of different measured samples, the temperature resistance performance of the composite gel samples was evaluated.

2.2.6 Microscopic structure analysis of composite gel system

The microscopic structure of the composite gel was observed using the Quanta 200F type environmental scanning electron microscope. The gel samples after freeze-drying were cut using a scalpel, and during the cutting process, the sample structure should be maintained properly. A small amount of the flat-cut samples to be tested was taken, placed on a sample platform coated with conductive glue, gold-plated, and then put into the sample chamber. After vacuuming, the samples were observed. Different magnification levels and positions could be selected as needed to observe the samples.

2.2.7 *Indoor Core Sealing Experiment*

(1) CO_2 Sealing Experiment

① Build the experimental device: According to the device diagram 1, build the indoor core sealing experimental device, ensuring the airtightness of the core holder;

② Core saturation with water: Place the experimental required core in a 90°C oven for drying for 24 hours, then take it out and weigh it. Record the dry weight, then place the core in the container, use the vacuum pump to vacuum the container for 12 hours, remove the gas in the core, then inject formation water into the container, keep the core in water for 12 hours, saturate the core with formation water, take it out and record the wet weight, calculate the pore volume;

③ Core saturation with oil: Mix crude oil and kerosene in a volume ratio of 4:1 evenly as the simulated crude oil for the oil displacement-sealing experiment. Place the core after saturation with water in the holder, connect the pipeline, set the oven temperature at 25°C, set the external pressure of the holder to 6 MPa, set the flow rate of the percolation pump to 0.2 mL/min, inject the prepared simulated oil into the holder until the end cylinder collects the simulated oil. Seal the end, saturate the core with simulated oil for 12 hours;

④ Primary gas displacement: After the core is saturated with oil, stabilize the external pressure at 6 MPa, set the percolation pump to 0.2 mL/min to inject CO_2 into the holder, collect and record the displaced oil volume in the end cylinder until the pressure and oil output stabilize, stop the injection;

⑤ Inject composite gel sample solution: Replace the six-way valve path, inject the composite gel sample solution into the holder, until the end cylinder receives the solution, seal the end, keep the composite gel sample solution in the holder reacting with CO_2 for 30 minutes;

⑥ Secondary gas displacement: After the CO_2-responsive worm-like micelles respond, inject CO_2 into the core holder again, observe the collected simulated oil volume and computer pressure reading in the end cylinder, until the pressure breaks and suddenly drops, end the oil displacement process.

(2) Water flooding blocking experiment

① Water flooding stage: Inject 0.2 mL/min of formation water into the formation, record the pressure changes during the water flooding process. When the water content of the produced liquid reaches 98%, it is considered that the water flooding is completed;

② Inject the composite gel sample solution: Inject the composite gel sample solution at a rate of 0.2 mL/min, record the pressure changes during the injection process. When the water content of the produced liquid reaches 98%, stop injecting the composite gel sample solution. At this time, close the inlet and outlet valves of the core holder to ensure that the holder is in a closed state, and turn on the heating switch. The artificial core is heated at 140°C until the composite gel sample solution inside the core completely gels;

③ Second water flooding stage: Again inject 0.2 mL/min of formation water, record the pressure changes during the water flooding process. When the water content of the produced liquid reaches 98%, it is considered that the second water flooding is completed.

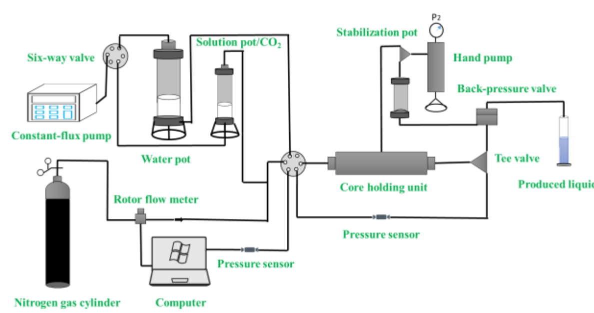

Fig. 1. Indoor core oil recovery and plugging experimental device

3. RESULTS

3.1 The responsiveness of the composite gel system to CO_2

Under the condition of controlling C_{NaOA} = 300 mmol·L^{-1}, a series of composite gel systems of DETA to NaOA with molar concentration ratios (r = C_{DETA}:C_{NaOA}) of 1, 1.Under the condition of controlling c_{NaOA} =300 mmol·L^{-1}, a series of composite gel systems of DETA to NaOA with molar concentration ratios (r = C_{DETA}:C_{NaOA}) of 1, 1.25, 1.5, 1.75, 2, 2.25, 2.5 were prepared. Then, CO_2 was bubbled into the samples at a rate of 80 mL/min for 2 minutes, and the samples were left to stand for 24 hours. Then, CO_2 was bubbled into the samples at a rate of 80 mL/min for 2 minutes, and the samples were left to stand for 24 hours. The apparent viscosity of the composite gel systems with different molar concentration ratios (r) before and after the CO_2 response was measured using the HAAKE MARS III rheometer, with the rotor speed set at 7.34 s^{-1}. The apparent viscosity of the composite gel systems with different molar concentration ratios (r) before and after the CO_2 response was measured using the HAAKE MARS III rheometer, with the rotor speed set at 7. The results are shown in Figure 2(a). As can be seen from Figure 2(a), the viscosity of each molar concentration ratio composite gel system was low before the CO_2 response, approximately 14 mPa·s. The viscosity of the composite gel system was lower in the r = 1 system after the CO_2 response, and it continued to increase as r continued to increase. It reached the maximum at r = 2, approximately 2.1×10^4 mPa·s, and then the viscosity decreased as r continued to increase. Subsequently, as r continued to increase, the viscosity decreased instead. Therefore, when $C_{DETA} : C_{NaOA} = 2$, the composite gel system had the maximum viscosity when CO_2 was introduced.

Under the condition of r = 2, the NaOA concentration (100, 200, 300, 400, 500 mmol·L^{-1}) was changed to prepare a series of composite gel systems. The apparent viscosity of the composite gel systems at 25°C before and after the CO_2 response was measured using the HAAKE MARS III rheometer. The results are shown in Figure 2(b). As can be seen from Figure 2(b), before the CO_2 response, the viscosity of the composite gel system was extremely low. After the CO_2 response of the composite gel system, as the molar concentration of NaOA gradually increased, the viscosity gradually increased, reaching the highest at C_{NaOA} = 400 mmol·L^{-1}. Subsequently, as the molar concentration of NaOA continued to increase, the viscosity of the system decreased instead. Therefore, the optimal molar concentration of NaOA was determined to be 400 mmol·L^{-1}.

Figure 2(c) shows the changes in pH value and conductivity over time of the sample solution of the composite gel system (r = 2, C_{NaOA} = 400 mmol·L-1) during the CO_2 introduction process. From Figure 2(c), it can be seen that the composite gel system exhibited a decrease in pH value and an increase in conductivity during the CO_2 introduction process. The pH decreased from 12.4 to approximately 7.2, and the conductivity increased from 6.8 ms/s to approximately 11.8 ms/s, indicating that the composite gel system underwent the protonation of DETA to produce $DETAH_2^{2+}$ during the CO_2 introduction process.

Figure 2(d) shows the viscosity changes of the composite gel system (r = 2, C_{NaOA} = 400 mmol·L^{-1}) during the CO_2 response process of the sample solution. In the process of introducing CO_2 into the composite gel system, the viscosity increased the fastest within the initial 20 seconds. Subsequently, as more CO_2 was introduced, the viscosity rose slowly, and it stabilized after reaching a viscosity of 1.88×10^4 mPa·s.

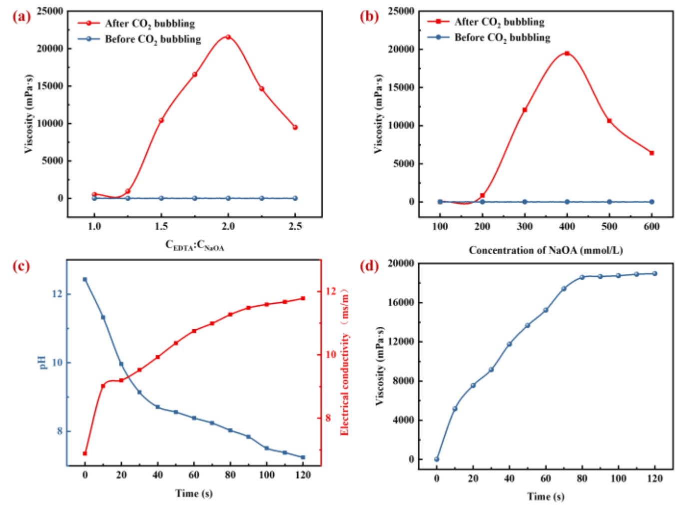

Fig. 2. The influence of CO_2 on the composite gel system

3.2 CO_2 Response Mechanism of the Composite Gel System

The hydrogen chemical shifts of DETA, NaOA, NaOA/DETA dissolved in heavy water, as well as those of DETA and NaOA/DETA after CO_2 bubbling are shown in Figure 3. From Figure 3, it can be observed that compared with the three nuclear magnetic resonance spectra of DETA, NaOA, and NaOA/DETA without CO_2 bubbling, the combination of NaOA and DETA did not significantly affect the hydrogen chemical shift. However, the hydrogen chemical shift of the DETA solution after CO_2 response was divided into four hydrogen species with larger chemical shifts, namely a1, a2, b1, and b2, at around 2.7 in a and b doublet. This chemical shift change confirmed that DETA did undergo protonation during the CO_2 response process, causing changes in the chemical shifts of various hydrogen species in the system. Among them, the hydrogen a2 and b2 belong to the by-product carbamate DETA-CO_2 and DETA-$(CO_2)_2$ produced during the protonation of the amino group, while the hydrogen a1 and b1 of the amino group that gained positive charge during protonation belongs to $DETAH_2^{2+}$.

From the integration of the area of the peaks, it can be concluded that the yields of these two products are equal. During the protonation process, the amino group acquires carbamoyl ester and protonated amino in the same ratio.By integrating the area of the peaks, it can be concluded that the yields of these two products are equal.This proves that after DETA undergoes protonation and combines with NaOA, it combines with the head group of NaOA, that is, $DETAH_2^{2+}$ combines with two NaOA- ions through electrostatic interaction to form a "pseudo-dual" surfactant [27], and then self-assembles to form worm-like micelles. This is the mechanism for the increase in viscosity of the composite gel system after CO_2 response.

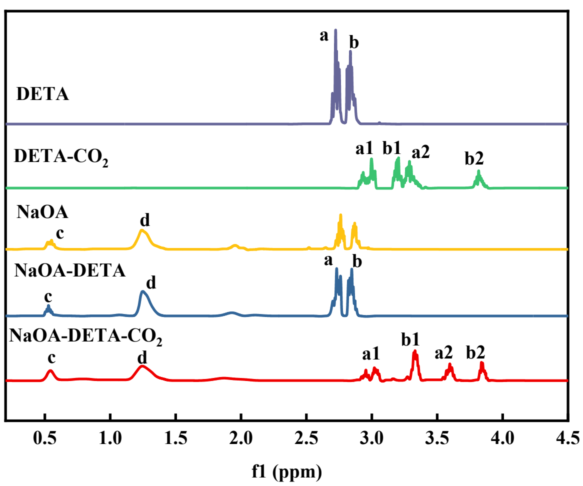

Fig.3. ^{1}H-NMR spectra of DETA, NaOA, and NaOA/DETA before and after CO_2 response

3.3 Rheological Responsiveness of the Composite Gel System to CO_2

Figure 4(a) shows the cyclic variation of viscosity of the composite gel system (r = 2, C_{NaOA} = 400 mmol·L^{-1}) solution during the alternating introduction of CO_2/N_2. In the cyclic introduction of CO_2/N_2 in the composite gel system, the viscosity fluctuated between 14 mPa·s and 1.8×10^4 mPa·s. Similarly, this reversible behavior maintained the highest viscosity unchanged during the three cycles, proving that the composite gel system can maintain multiple cycle stability at a higher viscosity during three cycles. The elastic modulus and viscous modulus of the composite gel system (r = 2, C_{NaOA} = 300 mmol·L^{-1}) within the stress scanning range of 0.01-100 Pa at a frequency of 1 Hz are shown in Figure 4(b). Within the stress scanning range of approximately 0.03 to 100 Pa, the elastic and viscous moduli of the composite gel system hardly change. At this frequency, the system is a viscoelastic fluid dominated by elasticity, with an elastic modulus of approximately 450 Pa and a viscous modulus of approximately 100 Pa. The dynamic rheological characteristic curves of the elastic modulus (G') and viscous modulus (G'') of the composite gel system at a fixed stress of 1 Pa with respect to frequency are shown in Figure 4(c). At low shear frequencies, the system is dominated by the viscous modulus. At a frequency of 0.15 Hz, the elastic modulus and viscous modulus intersect. After the frequency increases further, the system is dominated by the elastic modulus, and the relaxation time of the system is approximately 6.67 s. Figure 4(d) is the Cole-Cole diagram of the composite gel system, and the fitted curve is close to a semi-circle, indicating that the composite gel system is a worm-like micellar system.

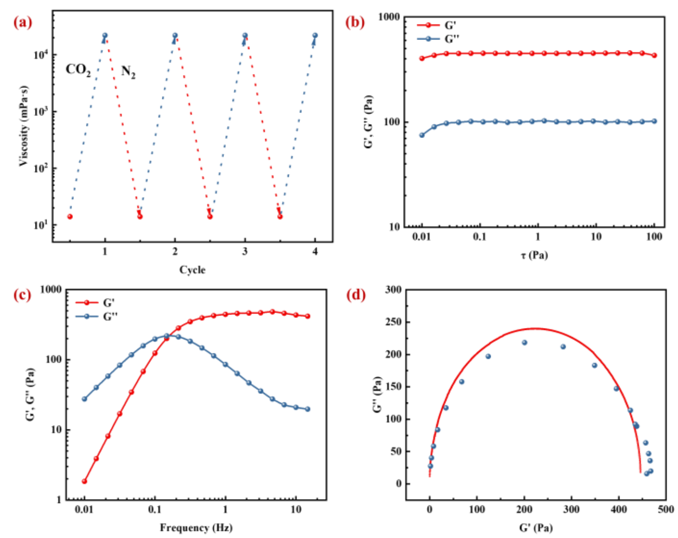

Fig.4. Rheological evaluation of the composite gel system

3.4 Temperature Response Mechanism of Composite Gel System

The prepared composite gel system was placed in a high-temperature oven at 140°C for a certain period of time. Then it was taken out and observed to check the gelation situation. The gelation situation is shown in Figure 5. As can be seen from Figure 5, the composite gel system was in a gray-white, flowable liquid state when it was prepared. It gelled at 140°C and was taken out from the vacuum storage bottle at 30 d, 90 d, 180 d, and 360 d to observe the gelation situation of the gel system. In different time periods, the system presented a solid gel state and no dehydration occurred. The strength was evaluated using the visual code method and was rated as level I. The experimental results show that the composite gel system has excellent long-term thermal stability in the 140°C high-temperature environment.

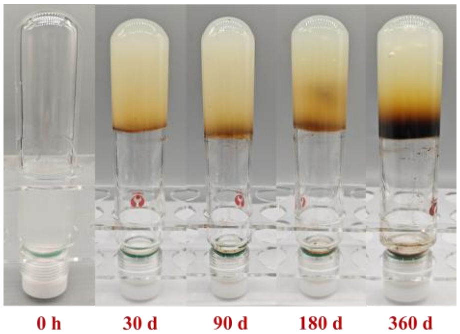

Fig.5. Gel formation effect of the composite gel system at 140°C

The in situ infrared experimental results of the composite gel system are shown in Figure 6. As can be seen from Figure 6, the characteristic functional groups of the composite gel system change with temperature. The relatively broad absorption peak at approximately 3300 cm^{-1} is the stretching vibration of the N-H of the amine in polyacrylamide and the N-H of the amine in the crosslinking agent polyethyleneimine. At 1672 cm^{-1}, it is the stretching vibration of the C=O of the acrylamide. At 1595 cm^{-1}, it is the bending vibration of the N-H of the amine in polyacrylamide. As the temperature increases, the peaks of the N-H of the amine in polyacrylamide and the amine in the crosslinking agent polyethyleneimine significantly weaken or even disappear. At the same time, the peaks of the C=O of the acrylamide in polyacrylamide and the amine peak at 1595 cm^{-1} also show a significant weakening phenomenon. Moreover, all these fully confirm that the amide group of polyacrylamide has undergone a crosslinking reaction with the amine in the crosslinking agent polyethyleneimine. What is more important to note is that this crosslinking reaction requires a certain temperature condition to be initiated. When the temperature is below 125°C, the crosslinking reaction hardly occurs or is very weak. Thus, it strongly proves that this gel system is a gel system with temperature-responsive characteristics.

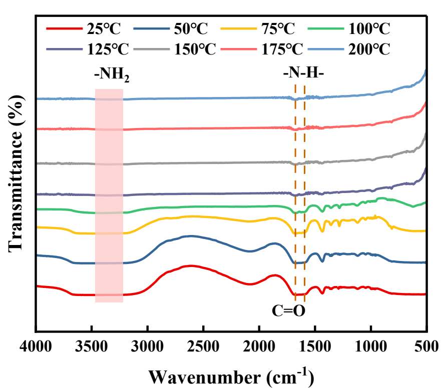

Fig.6. In-situ infrared spectrogram of the composite gel system

3.5 DSC Analysis of Composite Gel System

The differential scanning calorimetry analyzer can be used to more accurately determine the temperature at which the composite gel system decomposes. By adding different mass fractions of the reinforcing agent SiO_2 to the composite gel system and observing the peak temperature, the temperature resistance performance of the system can be evaluated. The experimental results are shown in Figure 7. As can be seen from Figure 7, with the increase in the mass fraction of the reinforcing agent SiO_2, the peak temperature gradually rises. The peak temperature of the system without adding the reinforcing agent was measured to be 131°C. When applied under the condition of 140°C oil reservoir, there is a risk of gel degradation, so the addition of the reinforcing agent is necessary to meet the requirement of withstanding 140°C temperature. When the mass fraction of the reinforcing agent SiO_2 is 2%, its peak temperature reaches 188°C, an increase of 57°C. Combining with the microstructure of the gel system with the added reinforcing agent SiO_2, it can be seen that the addition of the SiO_2 reinforcing agent further strengthens the intermolecular forces of the polymer, makes the cross-linked structure more compact, and is less prone to dehydration, which can significantly improve the thermal stability of the gel system [28].

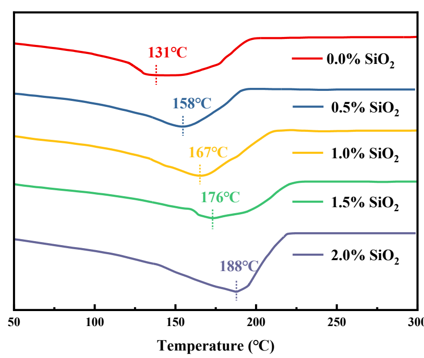

Fig.7. DSC curves of different quality fractions of SiO_2 composite gel systems

3.6 Microscopic Structure Analysis of Composite Gel System

The scanning electron microscope images of the composite gel system before and after gelation at a certain temperature are shown in Figure 8. Figure 8(a) and (b) are the electron microscope images of the composite gel system before gelation at 500x and 1000x magnification, respectively. It can be seen that the structure is loose, with only sheet-like thin layers. In contrast, the electron microscope images of the composite gel system after gelation at 500x and 1000x magnification (Figure 8(c) and (d)) show a tightly packed network structure. This is a cross-linked network structure formed by the cross-linking reaction between acrylamide and the cross-linking agent PEI at a certain temperature.

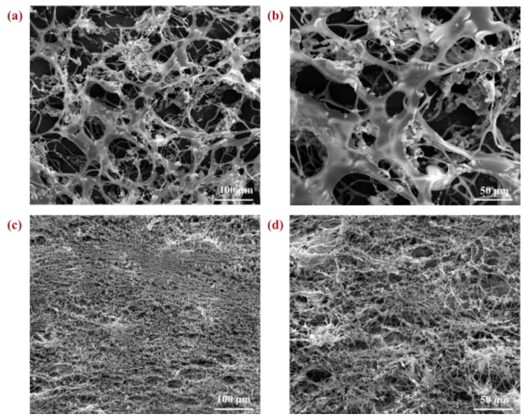

Fig.8. SEM images of the composite gel system before and after gelation (a) 500× before gelation; (b) 1000× after gelation; (c) 500× after gelation; (d) 1000× after gelation

3.7 Sealing Performance of Composite Gel System

The indoor core oil displacement and plugging experimental device as shown in Figure 1 was set up, and CO_2 plugging and water displacement plugging experiments were conducted on the composite gel system respectively. In the CO_2 plugging experiment, the injection speed of gas and liquid was both 0.2 mL/min. The porosity of the core was 18% and the permeability was 50 md. The cumulative injection volume of gas and liquid and the pressure difference of the core during the system's oil displacement process are shown in Figure 9(a). In the figure, Roman numerals I, II, and III represent the first gas displacement process, the process of injecting the micellar sample liquid, and the second gas displacement process respectively. From Figure 9(a), it can be seen that during the injection of CO_2 in stage I, the pressure difference remained at around 6 kPa and remained basically unchanged, indicating that there was no blocking material in the core model. In stage II, as the sample solution was continuously pumped in, the pressure continued to rise, and the injection was stopped after injecting 2 PV of the sample solution. Stage III was the second CO_2 gas displacement process. Compared with stage I, due to the formation of the composite gel system reacting with CO_2 to form worm-like micellar plugs, the pressure difference continued to increase until it reached 1643.53 kPa, and CO_2 broke through the plugging, with this pressure difference being much greater than that in stage I, and the plugging rate was approximately 99.61%. The pressure curve changes of the water flooding sealing experiment are divided into three stages, as shown in Figure 9(b). The first stage is the water injection stage for the artificial core. During this stage, the water injection pressures of the three curves fluctuate within the range of 412-432 kPa. The second stage is the injection of gel solution stage. The injection pressure starts to stabilize as the volume of the injected gel solution increases. The stable pressure during the injection of the gel solution is taken as the injection pressure of the gel solution, and the pressure of the injected composite gel solution is 15863 kPa. The third stage is the re-water injection stage. The injection pressure of the gel system increases with the increase of the injection water volume, but after the injection water breaks through the gel, the injection pressure begins to decrease. After the injection water breaks through the gel, it continues to be injected, and the injection pressure fluctuates before stabilizing. The injection pressure after the composite gel sealing is 37991 kPa. Through this pressure and the pressure of the first injection, the sealing rate of the system can be calculated. The sealing rate is 98.92%.

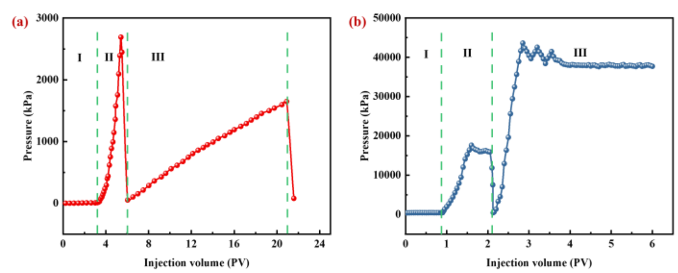

Figure 9 Pressure variation curve of the blocking experiment; (a) CO_2 flooding; (b) water flooding

4. CONCLUSIONS

In summary, based on the traditional CO_2-responsive worm-like micelle system, we introduced a temperature-responsive gel that can undergo cross-linking reactions at formation temperatures, thereby forming a composite gel system with dual responses to CO_2 and temperature. This composite gel system can achieve a viscosity of 2.1×10^4 mPa·s upon contact with CO_2, and can achieve a cyclic switching between high and low viscosities through N_2 and CO_2. The composite gel system undergoes cross-linking reactions at temperatures above 125°C, forming a non-flowing gel that can remain stable for 360 days at 140°C. Laboratory sealing experiments have shown that the composite gel system can achieve a CO_2 gas sealing rate of 99.61% and a water-driven sealing rate of 98.92%. This dual-response composite gel system for CO_2 and temperature has potential applications in the CCUS process for preventing CO_2 leakage and channeling.

ACKNOWLEDGEMENT

This study received support and funding from the National Natural Science Foundation of China (No. 52174047).

DECLARATION OF INTEREST STATEMENT

The authors declare that they have no known competing financial interests or personal relationships that could have appeared to influence the work reported in this paper. All authors read and approved the final manuscript.

REFERENCE

[1] E. Hanson, C. Nwakile, V.O. Hammed, Carbon capture, utilization, and storage (CCUS) technologies: Evaluating the effectiveness of advanced CCUS solutions for reducing CO2 emissions, Results in Surfaces and Interfaces.18(2025), 100381. https://doi.org/10.1016/j.rsurfi.2024.100381.

[2] B. Liang, C. Chen, C. Jia, C. Wang, X. Wang, Y. Zha, R. Wang, Z. Meng, H. Wang, Carbon capture, utilization and storage (CCUS) in oil and gas reservoirs in China: Status, opportunities and challenges, Fuel.375(2024), 132353. https://doi.org/10.1016/j.fuel.2024.132353.

[3] M. Zhao, H. He, C. Dai, Y. Sun, Y. Fang, Y. Liu, Q. You, G. Zhao, Y. Wu, Enhanced Oil Recovery Study of a New Mobility Control System on the Dynamic Imbibition in a Tight Oil Fracture Network Model, Energy & Fuels.32(3)(2018), 2908-2915. https://doi.org/10.1021/acs.energyfuels.7b03283.

[4] W. Yu, H.R. Lashgari, K. Wu, K. Sepehrnoori, CO2 injection for enhanced oil recovery in Bakken tight oil reservoirs, Fuel.159(2015), 354-363. https://doi.org/10.1016/j.fuel.2015.06.092.

[5] Q. You, H. Wang, Y. Zhang, Y. Liu, J. Fang, C. Dai, Experimental study on spontaneous imbibition of recycled fracturing flow-back fluid to enhance oil recovery in low permeability sandstone reservoirs, Journal of Petroleum Science and Engineering.166(2018), 375-380. https://doi.org/10.1016/j.petrol.2018.03.058.

[6] B. Yuan, Y. Su, R.G. Moghanloo, Z. Rui, W. Wang, Y. Shang, A new analytical multi-linear solution for gas flow toward fractured horizontal wells with different fracture intensity, Journal of Natural Gas Science and Engineering.23(2015), 227-238. https://doi.org/10.1016/j.jngse.2015.01.045.

[7] B. Yuan, D.A. Wood, W. Yu, Stimulation and hydraulic fracturing technology in natural gas reservoirs: Theory and case studies (2012–2015), Journal of Natural Gas Science and Engineering.26(2015), 1414-1421. https://doi.org/10.1016/j.jngse.2015.09.001.

[8] F. Lai, Z. Li, Q. Wei, T. Zhang, Q. Zhao, Experimental Investigation of Spontaneous Imbibition in a Tight Reservoir with Nuclear Magnetic Resonance Testing, Energy & Fuels.30(11)(2016), 8932-8940. https://doi.org/10.1021/acs.energyfuels.6b01324.

[9] L. Zhang, C. Pu, S. Cui, K. Nasir, L. Yang, Experimental Study on a New Type of Water Shutoff Agent Used in Fractured Low Permeability Reservoir, Journal of Energy Resources Technology-transactions of The Asme.139(2017), 012907.

[10] H. Zhao, Z. Ning, Q. Wang, R. Zhang, T. Zhao, T. Niu, Y. Zeng, Petrophysical characterization of tight oil reservoirs using pressure-controlled porosimetry combined with rate-controlled porosimetry, Fuel.154(2015), 233-242. https://doi.org/10.1016/j.fuel.2015.03.085.

[11] J. Wang, H. Liu, J. Zhang, Q. Meng, H. Liu, L. Ge, Z. Zhu, C. Liu, Experimental investigation on water flooding and continued EOR techniques in buried-hill metamorphic fractured reservoirs, Journal of Petroleum Science and Engineering.171(2018), 529-541. https://doi.org/10.1016/j.petrol.2018.07.051.

[12] Q. You, Q. Wen, J. Fang, M. Guo, Q. Zhang, C. Dai, Experimental study on lateral flooding for enhanced oil recovery in bottom-water reservoir with high water cut, Journal of Petroleum Science and Engineering.174(2019), 747-756. https://doi.org/10.1016/j.petrol.2018.11.053.

[13] A.M. Il'yasov, G.T. Bulgakova, Modeling of the Installation and Stability of Gel Barriers in Main Fractures, Journal of Applied Mechanics and Technical Physics.59(2)(2018), 359-367. https://doi.org/10.1134/S0021894418020207.

[14] C.A. Conn, K. Ma, G.J. Hirasaki, S.L. Biswal, Visualizing oil displacement with foam in a microfluidic device with permeability contrast, Lab on a Chip.14(20)(2014), 3968-3977. https://doi.org/10.1039/C4LC00620H.

[15] J. Wang, H. Liu, Z. Ning, H. Zhang, Experimental Research and Quantitative Characterization of Nitrogen Foam Blocking Characteristics, Energy &

Fuels.26(8)(2012), 5152-5163. https://doi.org/10.1021/ef300939j.
[16] L. Qinzhi, F.-y. Jin, H. Li, C. Wang, The Potential of a Novel Nano-fluid in Enhancing Oil Recovery, Energy & Fuels.30(2016). https://doi.org/10.1021/acs.energyfuels.6b00244.
[17] W. Li, D. Schechter, Using Polymer Alternating Gas to Maximize CO2 Flooding Performance, Trinidad and Tobago Energy Resources Conference, SPETT 2014 - Future Assets: Acquisition, Maintenance and Reliability.(2014). https://doi.org/10.2118/169942-MS.
[18] Y. Zhang, Y. Wang, F. Xue, Y. Wang, B. Ren, L. Zhang, S. Ren, CO2 foam flooding for improved oil recovery: Reservoir simulation models and influencing factors, Journal of Petroleum Science and Engineering.133(2015), 838-850. https://doi.org/10.1016/j.petrol.2015.04.003.
[19] H. He, Y. Wang, Z. Qi, X. Sun, Gelation Performance and Feasibility Study of an Environmental Friendly Improved Inorganic Aluminum Gel for Conformance Control Under Harsh Reservoir Conditions, Journal of Energy Resources Technology.139(1)(2017). https://doi.org/10.1115/1.4035512.
[20] A. Wilson, CO2 Low-Salinity Water Alternating Gas: A Promising New Approach for EOR, Journal of Petroleum Technology.67(2015), 84-86. https://doi.org/10.2118/0115-0084-JPT.
[21] U. Patil, A. Fihri, A.-H. Emwas, V. Polshettiwar, Silicon oxynitrides of KCC-1, SBA-15 and MCM-41 for CO2 capture with excellent stability and regenerability, Chemical Science.3(7)(2012), 2224-2229. https://doi.org/10.1039/C2SC20356A.
[22] S.R. Raghavan, E.W. Kaler, Highly Viscoelastic Wormlike Micellar Solutions Formed by Cationic Surfactants with Long Unsaturated Tails, Langmuir.17(2)(2001), 300-306. https://doi.org/10.1021/la0007933.
[23] H. Afifi, G. Karlsson, R.K. Heenan, C.A. Dreiss, Structural transitions in cholesterol-based wormlike micelles induced by encapsulating alkyl ester oils with varying architecture, Journal of Colloid and Interface Science.378(1)(2012), 125-134. https://doi.org/10.1016/j.jcis.2012.04.014.
[24] Y. Liu, P.G. Jessop, M. Cunningham, C.A. Eckert, C.L. Liotta, Switchable Surfactants, Science.313(5789)(2006), 958-960. https://doi.org/doi:10.1126/science.1128142.
[25] X. Su, M.F. Cunningham, P.G. Jessop, Switchable viscosity triggered by CO2 using smart worm-like micelles, Chemical Communications.49(26)(2013), 2655-2657. https://doi.org/10.1039/C3CC37816K.
[26] Y. Zhang, Y. Feng, Y. Wang, X. Li, CO2-Switchable Viscoelastic Fluids Based on a Pseudogemini Surfactant, Langmuir.29(13)(2013), 4187-4192. https://doi.org/10.1021/la400051a.
[27] Y. Zhang, Y. Feng, J. Wang, S. He, Z. Guo, Z. Chu, C.A. Dreiss, CO2-switchable wormlike micelles, Chemical Communications.49(43)(2013), 4902-4904. https://doi.org/10.1039/C3CC41059E.
[28] Y. Liu, C. Dai, K. Wang, C. Zou, M. Gao, Y. Fang, M. Zhao, Y. Wu, Q. You, Study on a Novel Cross-Linked Polymer Gel Strengthened with Silica Nanoparticles, Energy & Fuels.31(9)(2017), 9152-9161. https://doi.org/10.1021/acs.energyfuels.7b01432.